Revista Brasileira de Ciências Ambientais
Brazilian Journal of Environmental Sciences

Influence of climatic phenomena and deforestation on hydroenvironmental fragility, Gurupi River watershed, Northern Brazil

Influência de fenômenos climáticos e do desmatamento na fragilidade hidroambiental, bacia hidrográfica do Rio Gurupi, Norte do Brasil

Dênis José Cardoso Gomes[1], *Norma Ely Santos Beltrão*[1], *Aline Maria Meiguins de Lima*[2]

ABSTRACT

In recent decades, climatic and anthropogenic pressures have caused serious environmental problems. The joint analysis of geo-environmental variables, through geoprocessing techniques, can support the estimation of the contribution of each environmental component to hydro-environmental fragility (HF). The aim of this work was to analyze the contribution of climatic phenomena and deforestation in the HF of the Gurupi River Watershed (GRW). Precipitation data were extracted from the Climate Hazards Group InfraRed Precipitation with Stations (CHIRPS); land use and cover were obtained from the MapBiomas Project; drainage network was acquired from the National Water and Sanitation Agency (ANA); slope data were gathered from the National Institute for Space Research (INPE); soil data were obtained from the Brazilian Agricultural Research Corporation (EMBRAPA); geomorphological units were extracted from the Brazilian Institute of Geography and Statistics (IBGE); and rock data were based on the Geological Survey of Brazil (CPRM). For the mapping of HF, the Analytic Hierarchy Process (AHP) was adopted to weigh the importance of each variable in four extreme precipitation year scenarios (1989, 2012, 2015, and 2019). It was observed that spatial precipitation is considerably different in extreme years. Results showed that deforestation has increased over the years; and that static geo-environmental variables (drainage, slope, soils, geomorphological units, and rocks) have larger feature domains that favor the increase of HF in the GRW. The HF of the GRW showed significant differences in the analyzed scenarios. Policies and environmental conservation programs are needed in the GRW.

Keywords: extreme years; land use and land cover; geosystems.

RESUMO

Nas últimas décadas as pressões climáticas e antrópicas vêm causando sérios problemas ambientais. A análise conjunta de variáveis geoambientais, por meio de técnicas de geoprocessamento, pode subsidiar a estimativa da contribuição de cada componente ambiental na fragilidade hidroambiental (FHA). O objetivo do trabalho foi analisar a contribuição dos fenômenos climáticos e do desmatamento na FHA da Bacia Hidrográfica do rio Gurupi (BHG). Utilizaram-se dados de precipitação do *Climate Hazards Group InfraRed Precipitation with Stations* (CHIRPS); o uso e cobertura do solo foram obtidos do Projeto MapBiomas; a rede de drenagem foi adquirida na Agência Nacional de Águas e Saneamento Básico (ANA); a declividade foi obtida do Instituto Nacional de Pesquisas Espaciais (INPE); os dados de solos foram obtidos da Empresa Brasileira de Pesquisa Agropecuária (EMBRAPA); foram consideradas as unidades geomorfológicas do Instituto Brasileiro de Geografia e Estatística (IBGE) e os dados de rochas do Serviço Geológico do Brasil (CPRM). Para o mapeamento da FHA, adotou-se a *Analytic Hierarchy Process* (AHP) com a finalidade de ponderação de importância para cada variável, em quatro cenários de anos extremos de precipitação (1989, 2012, 2015 e 2019). Observou-se que a precipitação espacial é consideravelmente diferente nos anos extremos. Os resultados mostram que o desmatamento aumentou ao longo dos anos; que as variáveis geoambientais estáticas (drenagem, declividade, solos, unidades geomorfológicas e rochas) possuem maiores domínios de feições que favorecem o aumento da FHA na BHG. A FHA da BHG apresentou diferenças significativas nos cenários analisados. A BHG necessita de políticas e programas de conservação ambiental.

Palavras-chave: anos extremos; uso e cobertura do solo; geossistemas.

[1]Universidade do Estado do Pará – Belém (PA), Brazil.

[2]Universidade Federal do Pará – Belém (PA), Brazil.

Correspondence address: Dênis José Cardoso Gomes – Travessa Doutor Enéas Pinheiro, 2626 – Marco – CEP: 66095-100 – Belém (PA), Brazil.
E-mail: deniss.feg@gmail.com

Conflicts of interest: the authors declare no conflicts of interest.

Funding: Fundação Amazônia de Amparo a Estudos e Pesquisas – FAPESPA (Amazon Foundation for Studies and Research Support)

Received on: 05/08/2023. Accepted on: 08/10/2023.

https://doi.org/10.5327/Z2176-94781621

Introduction

Generally, environmental problems are caused by hydroclimatic forcings that lead to extreme scenarios of water excess or scarcity (Costa and Blanco, 2018; Towner et al., 2020). The culprits behind this situation are climatological phenomena that should be studied and monitored in order to mitigate the impacts of potential natural disasters; therefore, information about these natural events contributes to preventing their effects on society (Aguirre-Ayerbe et al., 2020). It is necessary to understand how these natural factors operate and their effects on the environment.

Climatic phenomena are natural events that influence precipitation in the Amazon region (Towner et al., 2020). This means that in a given year, under the influence of these phenomena, precipitation levels can significantly decrease and/or increase (Costa and Blanco, 2018). When this occurs, it is referred to as extreme events, and the period of their occurrence can be classified as extreme years (Jorge and Lucena, 2018). Associated with these extreme events, climatic mechanisms are processes of ocean-atmosphere interaction that enable the formation of climate phenomena (Nóbrega et al., 2016; Pezzi et al., 2016). Accoring to Kelman (2019), among the climatic mechanisms contributing to the occurrence of extreme precipitation years, the El Niño-Southern Oscillation (ENSO) stands out. ENSO is composed of phases known as El Niño (EN) and La Niña (LA), which have decreasing (EN) and increasing (LA) effects on precipitation in many parts of the northern Brazilian region (Córdova et al., 2022). The Atlantic dipole (AD) is another climatic mechanism consisting of positive (AD^+) and negative (AD^-) phases, which intensify precipitation variability in the Amazon (Jahfer et al., 2017).

In addition to the atmospheric variable, precipitation, the terrestrial surface and its landscape dynamics also influence terrain fragility, leading to increased environmental problems related to unregulated human occupation and the extensive transformation of the Amazon's natural landscape (Silva et al., 2022). The environmental changes result from natural events (Huguenin and Meirelles, 2022) as well as anthropogenic interventions for agricultural purposes, especially in eastern Amazonia (Silva et al., 2022). The effects of anthropization processes in eastern Amazonia are corroborated by the increased environmental degradation caused by changes in land use and land cover (LULC) in a hydrographic basin in the same region (Silva et al., 2021).

The term "land use and land cover" is widely used in discussions about anthropogenic interactions with the natural environment. Considered an important component, changes in LULC are associated with environmental changes and represent the dynamics of anthropogenic activities (Marengo et al., 2022), where deforestation is an example, contributing to increased soil erosion (Teshome et al., 2022). This type of environmental degradation in eastern Amazonia is a reflection of technological advancement and the economy, with increasing environmental exploitation (Huguenin and Meirelles, 2022). This places territorial planning as a priority because factors (climate, LULC) that amplify natural terrain fragility can lead to soil instability due to degradation (Dias and Lima, 2020). In this context, anthropogenic influences such as agricultural and livestock activities are the aggravating factors that have had the greatest impact on the environment in recent decades (Silva et al., 2022).

It is pertinent to consider precipitation and LULC as dynamic geo-environmental variables since they exhibit characteristics of high spatiotemporal variability (Paca et al., 2020; Marengo et al., 2022). However, these are external forcings on the terrain, as there are also internal components considered static geo-environmental variables due to their slow spatial and temporal changes (Faisal and Hayakawa, 2022; Musso et al., 2022). Internal forcings are related to landforms, geomorphological features, rock formations, and soil properties. Thus, Dias and Lima (2020) developed hydro-environmental zoning and analyzed the effects of precipitation and LULC associated with static geo-environmental variables on the fragility of an Amazonian watershed.

Given the impacts of external forcings such as dynamic variables on areas composed of static variables, it is important to investigate how the combination of climatic and anthropogenic pressures (Marengo et al., 2022) is affecting hydro-environmental fragility (HF) at the level of watersheds. Assuming that watersheds are sensitive environmental systems to changes in their landscape (Tricart, 1977; Lira et al., 2022), it is interesting to analyze HF in a watershed in the far eastern Amazonia, as it is a region where its natural landscape has been heavily altered by anthropogenic actions, in addition to being marked by the influence of climatic phenomena.

However, despite numerous studies addressing this theme, there is a gap in the scientific literature regarding the differences in HF in different climatic and deforestation scenarios in a transitional watershed between biomes. Thus, the objective of this study was to analyze the contribution of climatic phenomena and deforestation to HF in the Gurupi River Watershed (GRW).

Materials and Methods

Study area

The GRW covers a territorial extension of approximately 35,875.0 km^2 and has a population of 392,601 inhabitants (ANA, 2015). It is located in the northern region of Brazil in the eastern Amazonia (Figure 1), encompassing the cross-border area of the states of Pará (PA) and Maranhão (MA). Within the GRW boundaries, there are 11 municipal seats and its area includes 14 municipalities. In terms of socio-environmental aspects, the GRW consists of conservation units (CUs) to the east of the Gurupi Upper (GU), with 1,571.8 km^2; indigenous lands (ILs), covering approximately 5,177.4 km^2 in the transition

zone between the GU and Gurupi Lower (GL) sub-basins; and permanent protection areas (PPAs), with 126.2 km² along the coastline, near the mouth of the Gurupi River.

The GRW landscape is characterized by the transition between the Amazon and savannah biomes, with a predominance of dense Amazon rainforests and areas of savanna formations (MapBiomas Project, 2022). The topography of GRW is marked by plateaus (192–336 m) in the southern region (GU), where the Serra do Gurupi is located and the Gurupi River originates, stretching for 700 km until GL, where plains (1–144 m) predominate and the river flows into the estuarine zone of the Atlantic Ocean. The hydrographic system of GRW also includes tributaries such as the Açailândia, Itinga, Gurupizinho, Piriá, and Uraim rivers (ANA, 2015).

The climatic conditions of the region are characterized by relatively high annual precipitation of 1,450–2,650 mm, a minimum air temperature of 24°C and maximum of 33°C, with low annual temperature variation, high relative air humidity of 85%, regular evapotranspiration of 1,400 mm, and low wind speed of 2 m/s, with a well-defined direction from the northeast (INMET, 2022).

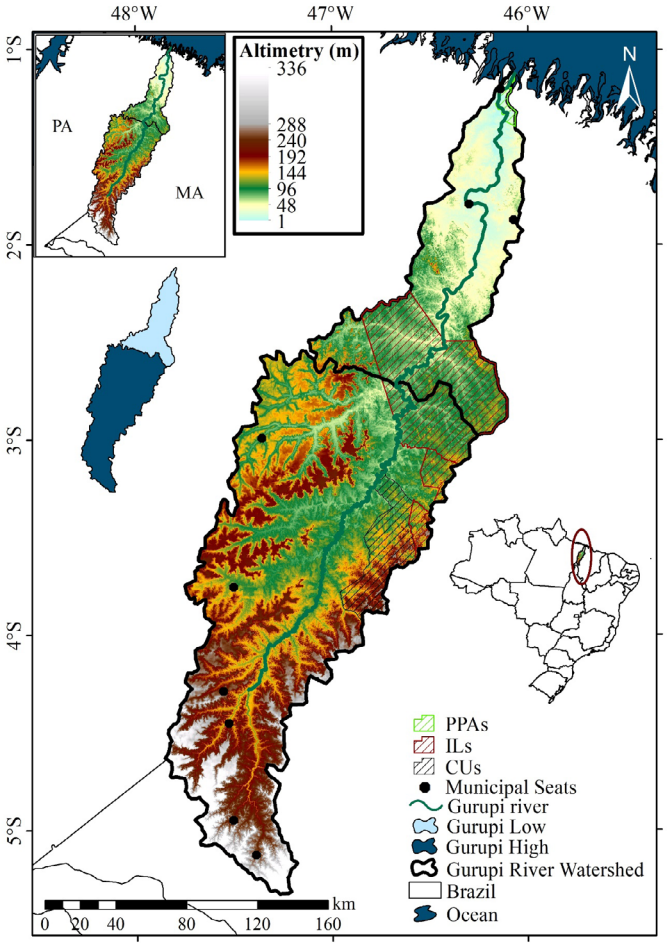

Figure 1 – Location of the study area: Gurupi River Watershed.
PPAs: permanent protection areas; ILs: indigenous lands; CUs: conservation units.

Data Acquisition

For rainfall spatialization, the dataset suggested by Funk et al. (2015) was used – the Climate Hazards Group InfraRed Precipitation with Stations (CHIRPS, 2022) – with a spatial resolution of 0.05° (~ 5 km). Cartographic products for other geo-environmental variables, such as LULC, were obtained from the MapBiomas Project (2022). The drainage network was acquired from the National Water and Sanitation Agency (ANA, 2022). Slope data were gathered from geomorphometric data provided by the National Institute for Space Research (INPE, 2022). Soil types were based on the classification of the EMBRAPA soil map (2022). Geomorphological units were extracted from the Brazilian Institute of Geography and Statistics (IBGE, 2022), and rock types were based on the geological map from the Geological Survey of Brazil (CPRM, 2022).

Data processing

For this study, the methodology of França et al. (2022) was employed. Initially, cartography was generated within a geographic information system (GIS), utilizing various geo-environmental variables (rainfall, LULC, slope, soils, rocks, geomorphology, and drainage density) with the aim of obtaining the product representing HF (fragility to hydrological alterations). The analysis criteria followed the methodology proposed by Saaty (1980) and further developed by Ross (1994), which was also subsequently applied by Bacani et al. (2015), Dias and Lima (2020), and França et al. (2022). Criteria weighting was accomplished using the Analytic Hierarchy Process (AHP) method (França et al., 2022). After a review of the scientific literature, consultations were conducted with experts qualified in research involving the geo-environmental variables studied in this work to analyze how each component contributes to the increase or decrease in HF and make an empirical decision regarding the impact of each variable (Sinshaw et al., 2021).

Rainfall was spatialized as done by França et al. (2022), but it was adapted to utilize precipitation data only from years influenced by climatic phenomena originating from the Atlantic and Pacific oceans (Gomes et al., 2022). The extreme years analyzed were: 1989 (LN: La Niña), 2012 (DA^+: positive Atlantic Dipole), 2015 (EN: El Niño), and 2019 (AD^-: negative Atlantic dipole). In all of these years, the most intense episodes of their respective phenomena occurred, favoring increases and decreases in precipitation (Gomes et al., 2022). Additionally, this meteorological component was referred to as a dynamic variable, as precipitation in the study region exhibits high spatiotemporal variability. It was considered one of the main components for the final calculations. Another geo-environmental component, also referred to as a dynamic variable, was the LULC, due to the rapid changes in space and time caused by accelerated deforestation. Therefore, the years of LULC (1989, 2012, 2015, and 2019) were selected to represent different HF scenarios for each year.

The components slope, soils, rocks, geomorphological units, and drainage density were referred to as static variables because their respective spatiotemporal changes are slow. It is worth noting that drainage density was considered static from a cartographic perspective as drainage is generally closely related to precipitation variability and consequently undergoes changes concomitantly with the pluviometric regime. Another point to highlight is that drainage density was calculated based on the kernel method (Siqueira et al., 2017).

Following these steps, the construction of HF scenarios (Equation 1) proceeded with the insertion of spatialized products of the geo-environmental variables into a raster calculator tool, using their respective weights acquired through the AHP. The HF class intervals were adapted from Bacani et al. (2015) and range from 0 to 1, as follows: low (0–0.27), medium (0.28–0.66), and high (0.67–1.00). Values close to zero indicate more stable and less fragile terrain with respect to soil erosion. As values approach one, the area becomes more susceptible to erosive processes.

$$HF = \frac{\Sigma(p*va)}{n} \quad (1)$$

Where:
HF: hydro-environmental fragility;
p: AHP weight;
va: environmental variables;
n: total number of variables under analysis.

The characteristics of each analyzed geo-environmental variable were considered for their classification and weighting criteria (Table 1). Three levels of classes (low, medium, and high) are described to indicate the degree of influence of the variables on the environmental degradation process. Furthermore, the class levels aim to represent the values of certain variables (precipitation, slope, and drainage density) and categories or types of other variables (LULC, geomorphological units, soils, and rocks).

For the analyzed geo-environmental variables (precipitation, LULC, slope, soils, rocks, geomorphology, and drainage density), potential risks were calculated, and weights were assigned based on the degrees of environmental degradation (rainfall volume, land use forms, types) that each geo-environmental component contributes to regional morphogenesis, e.g., to the erosive processes of the GRW as described in Table 2.

Table 1 – Classifications and respective criteria adopted for the hydro-environmental fragility of the Gurupi River Watershed.

Classes HF	Criteria						
	Rainfall (mm)	LULC	Geomorphological Units	Slope (Degrees)	Drainage Density (km/km²)	Soils	Rocks
Low	< 1,500	Forest, Savannah Formation, Reforestation, Body Water, Mangrove and Flooded Area	Plains, Surfaces and Mangroves	< 8.6	< 10	Ultisols	Amphibolites, Gneisses-Tonalite, Metamorphic Grades, Metadacites, Mica-Quartz, Muscovite-Granite, Tonalite-Granite and Shale-Phyllites
Medium	1,501 > 3,000	Urban Area Mining and Fields	Tablelands	8.7 > 27	10 > 20	Gleysols and Plinthosols	Sand-Clay, Sediments Muddy and Sand
High	> 3,000	Agriculture and Pasture	Highlands, Hills and Depressions	> 27	> 20	Latosols	Archosean Sand, Gravel, Sandstone, Biocalcirrudites and Clay-Peat-Silt-Graywacke

Source: França et al. (2022).
HF: hydro-environmental fragility; LULC: land use and land cover.

Table 2 – Classifications, weights, and descriptions of the hydro-environmental fragility of the Gurupi River Watershed.

Classes	Weights	Description
Low	1	Potential soil erosion resistance and morphogenesis equilibrium
Medium	2	Potential moderate fragility marked by the transition to morphogenesis instability due to the effects on the terrain of some analyzed geo-environmental variables
High	3	Potential unstable areas extremely sensitive to the action of morphodynamic factors that can cause soil erosion and environmental degradation in these types of terrain

Source: França et al. (2022).

To verify the consistency of the AHP assessment, the consistency index (CI) and the consistency ratio (CR) were calculated, described respectively in Equations 2 and 3. Acceptable values were obtained with CI (0.08) and CR (0.06), indicating the reliability of the variable weights. The steps of the adopted procedures are presented in Figure 2.

$$CI = \frac{\lambda_{max} - n}{n-1} \quad (2)$$

Where:
CI: consistency index;
λmax: arithmetic mean of the eigenvector;
n: number of analyzed variables.

$$CR = \frac{CI}{RI} \quad (3)$$

Where:
CR: consistency ratio;
CI: consistency index;
RI: random index.

Results

Fragilities of dynamic variables: years (1989, 2012, 2015, 2019)

Figure 3 presents the spatialized fragilities regarding precipitation in extreme years. Under the influence of LN (1989), the fragility was classified as moderate and predominant in the GL with 34,800.5 km² (99.1%), except for a small area of 314.2 km² (0.9%) to the northeast in the GL that exhibited high precipitation volume and high fragility.

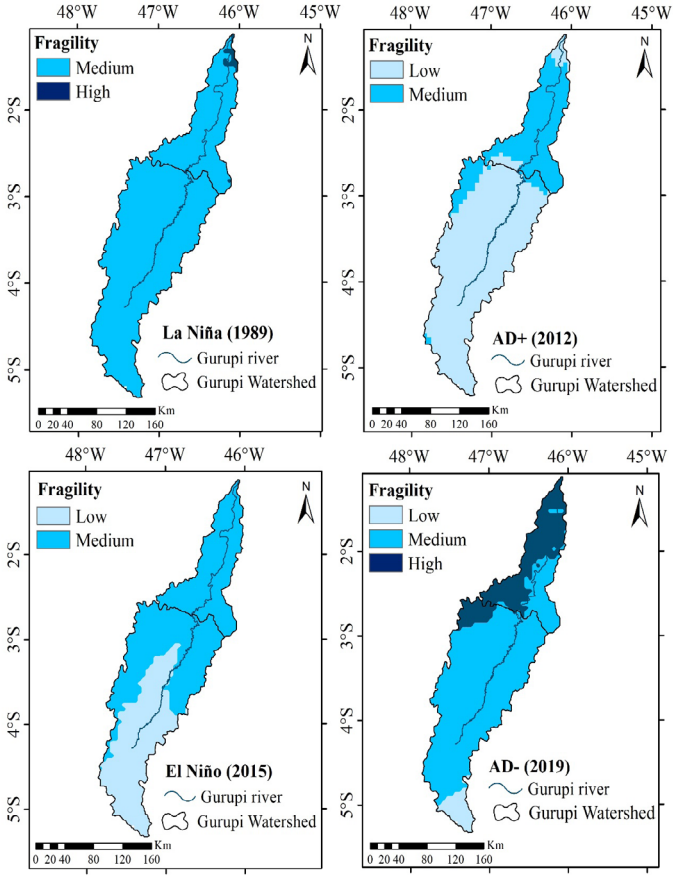

Figure 3 – Pluviometric fragility (1989, 2012, 2015, and 2019): Gurupi River Watershed.
AD⁺: positive Atlantic dipole; AD⁻: negative Atlantic dipole.

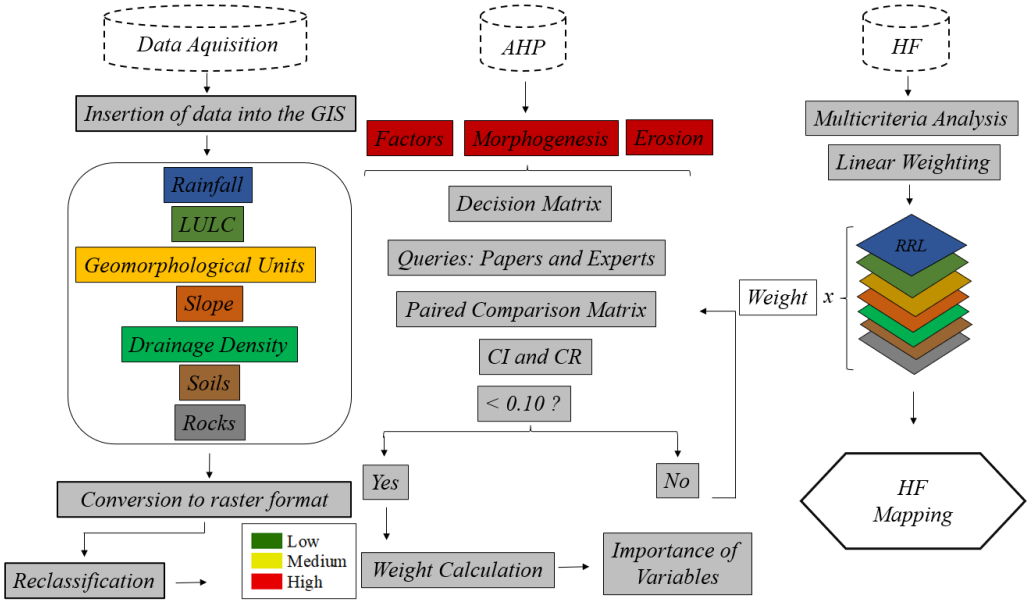

Figure 2 – Flowchart of the methodological steps of hydro-environmental fragility.
AHP: Analytic Hierarchy Process; HF: hydro-environmental fragility. GIS: geographic information system; LULC: land use and land cover; CI: consistency index; CR: consistency ratio; RRL: reclassified raster layers.

However, in the scenario of EN (2015), low fragility was observed to the south, in the GU with an area of 12,374.8 km² (35.3%), and a moderate classification in the central-northern part with 22,696.4 km² (64.7%), covering the entire GL region.

The extreme years related to the phases of the AD showed very different spatial distributions of fragilities. During the AD⁺ period (2012), precipitation fragility was classified as low in most GU with 24,308.0 km² (69.4%) along with a small area near the mouth of the Gurupi River. The GL was classified as moderate fragility with 10,712.4 km² (30.6%). Meanwhile, AD⁻ (2019) was the only extreme year where the three fragility classifications were observed. The low fragility zone was located in the extreme south of GU with 1,626.0 km² (4.6%). The central sector of GRW extending to the southeast of GL was classified as moderate fragility, covering the largest area with approximately 25,464.8 km² (72.6%). Additionally, high fragility was detected in the north-northwest axis region with 7,987.0 km² (22.7%).

The spatialized fragilities (Figure 4) regarding LULC (1989, 2012, 2015, 2019) showed anthropogenic actions impacting different parts of GRW. In 1989, there was a predominance of low-fragility areas with 26,939.1 km² (77.1%), mainly in GL and the southeastern sector of GRW. In this same period, there were still regions of 70.1 km² (0.2%) with moderate fragility near the river mouth and 7,913.1 km² (22.6%) classified as high fragility concentrated in the south-southwest sector.

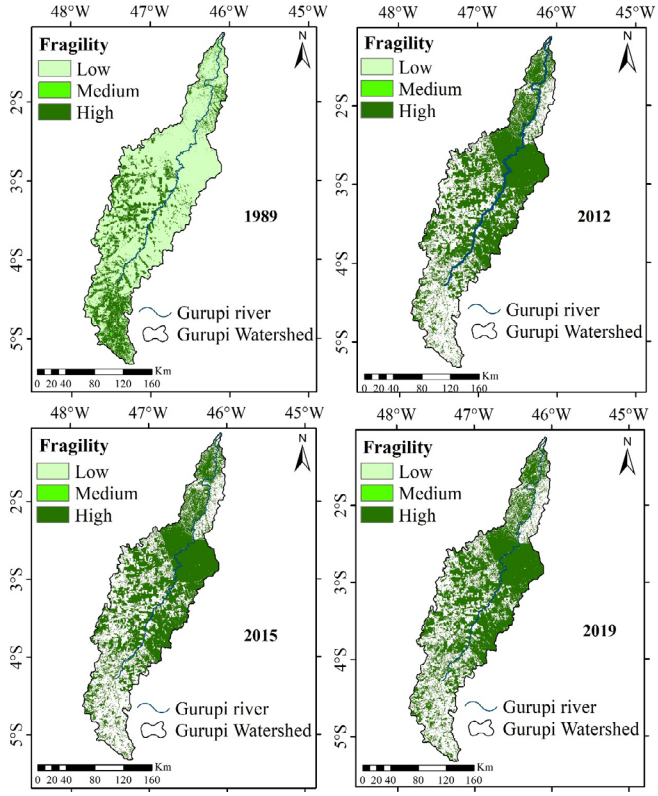

Figure 4 – Land use and land cover fragility (1989, 2012, 2015, and 2019): Gurupi River Watershed.

In 2012, there was a decline in areas with low fragility (20,598.1 km²; 59.0%). Concurrently, the expansion of moderate (103.9 km²; 0.3%) and high fragility (14,220.3 km²; 40.7%) zones was possibly evidence of environmental degradation, reflecting regional deforestation. Although low fragility continued to predominate in GRW in the years 2015 (20,385.3 km²; 58.4%) and 2019 (20,912.4 km²; 59.9%), the increase in areas classified as high fragility also remained significant in 2015 (14,430.3 km²; 41.3%) and 2019 (13,888.3 km²; 39.7%). This indicates the ongoing advancement and agricultural pressure exerted on the forest formations of GRW.

The fragility of geo-environmental variables in GRW was spatialized in Figure 5. River fragility showed a low classification in a small area of 83.4 km² (0.2%) in the extreme east of GRW, whereas moderate fragilities were observed to the south in GU and in a large part of GL, covering approximately 13,528.4 km² (38.7%). The largest zones were classified as high fragility with 21,342.4 km² (61.0%) and were predominantly located in the central part of GRW, with a small area to the north in GL.

Geomorphological fragility had the smallest areas in the low (2,332.4 km²; 6.7%) and medium (7,710.5 km²; 22.1%) categories, concentrated in the northeast and northwest, respectively. However, GRW was dominated by regions with high fragility (24,796.8 km²; 71.1%), especially in GU and a large part of GL. Some geomorphological features may be related to the slope of the land surface, as such landforms have very rugged terrain. Thus, the clinographic fragility of GRW was marked by the dominance and balance between areas classified as low (17,542.0 km²; 50.2%) and medium (16,673.9 km²; 47.7%), distributed throughout all parts of GRW. Areas with high fragility (705.7 km²; 2.0%) were lower and concentrated in the central region and some points to the east.

In soil composition, although low pedological fragility (4,727.4 km²; 13.6%) was the smallest area (GL, east, and south), the spatial distribution of soil fragilities also exhibited balance with respect to medium class (13,190.1 km²; 37.8%) to the north and high class (16,912.9 km²; 48.5%) in the western part, showing the degradation of GRW in relation to this environmental component. In GRW, the lowest areas of lithological fragility were low (4,350.3 km²; 12.5%) in GL and medium (6,727.8 km²; 19.3%) in the southwest region. Meanwhile, high fragility covered 23,758.9 km² (68.2%) in the eastern sector.

Figure 6 highlights HF, representing the effects of extreme years and their different forms of LULC. In 1989, low HF (0.21) was concentrated in the northeast of GL, possibly influenced by LULC associated with some geo-environmental variables, where the combination of these components favored stability. Medium HF (0.40) was observed to the south and southwest of GRW, mainly in the Paragominas municipality region. These risk zones are exacerbated due to the LN phenomenon, which contributes to increased precipitation in some deforestation areas dominated by drainage density and soil types, intensifying HF.

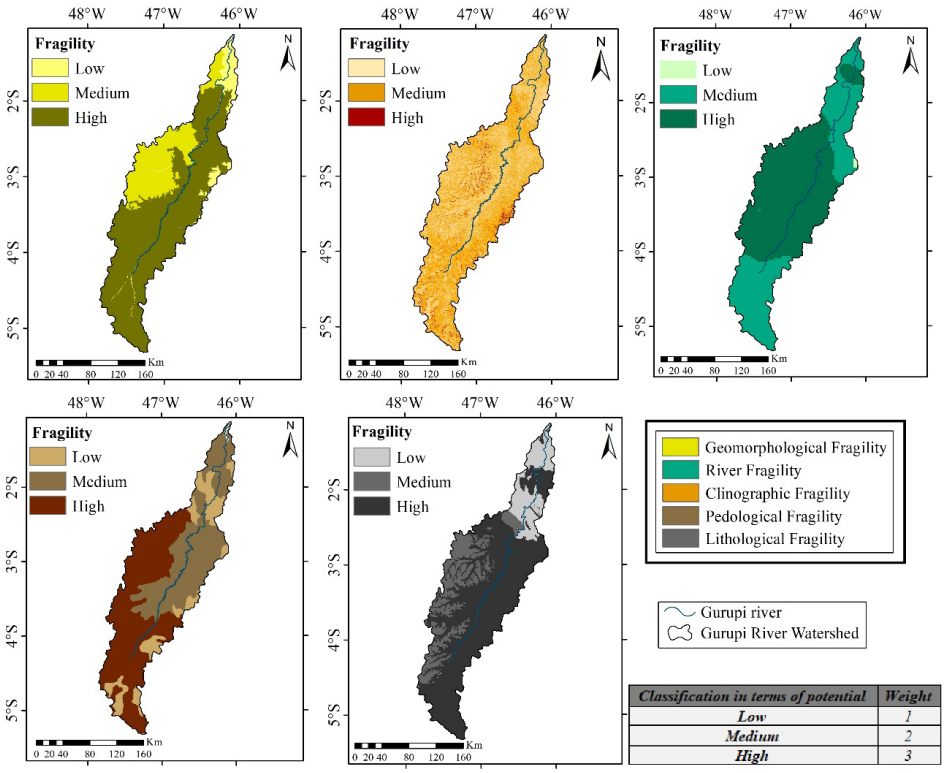

Figure 5 – Fragility of static variables: Gurupi River Watershed.

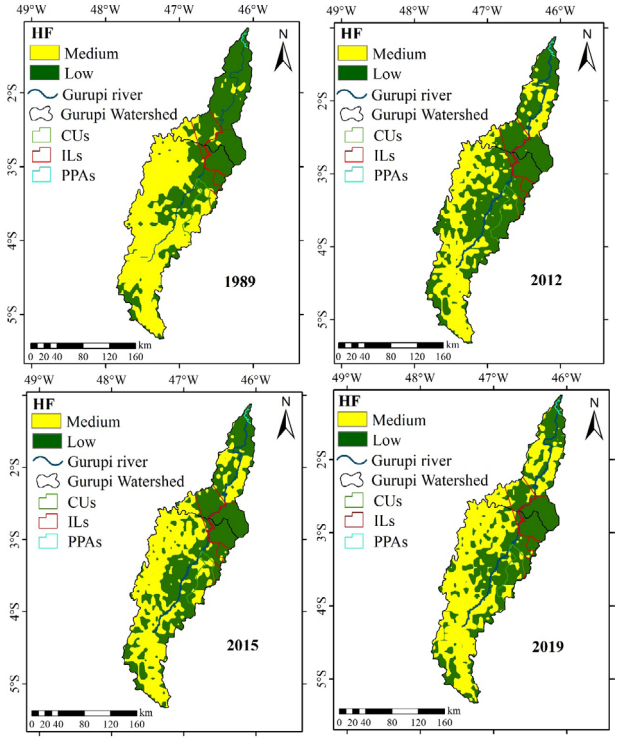

Figure 6 – Hydro-environmental fragility (1989, 2012, 2015, and 2019): Gurupi River Watershed.
CUs: conservation units. ILs: indigenous lands; PPAs: permanent protection areas.

Another scenario of an extremely rainy year was in 2019, when AD⁻ influenced the high rainfall volume above normal, combined with LULC in some areas of geo-environmental variables. This contributed to the moderate HF index (0.41) to the northwest of GRW, with emphasis on some points in GL and particularly near the headwaters of the Gurupi River. It is worth noting that in this year, there was a decrease in low (0.19) HF areas in GL.

In dry years like 2012, the reduction in rainfall caused by the AD⁺ phenomenon decreased the impacts on GRW with a low HF (0.17). Deforestation advanced significantly during this period in the southern, eastern, and some points in the GL sectors. These deforestation points occurred in regions with high geomorphological, clinographic, pedological, and lithological fragility, making the removal of vegetation cover more detrimental in these areas. Meanwhile, the zones of high HF (0.39) to the east were intensified by deforestation in areas of high fluvial and pedological fragility.

In 2015, the EN also favored a reduction in precipitation in GRW, directly reducing the effects of this variable with low HF (0.20) during this period. However, the zones of medium HF (0.42) observed in the eastern sector were the effects of LULC, where extensive forest areas were devastated for the use of large land areas for agriculture and pasture activities. This is an aggravating factor, as it occurred in naturally unstable zones, especially due to high fluvial and pedological fragilities.

Discussion

While precipitation in GRW exhibited significant differences in extreme years, the highest volume of rainfall was concentrated in GL in all the years analyzed under the influence of climatic phenomena. This suggests that GRW is possibly influenced by more than one rainfall regime, which may be associated with the region's location in a biome transition zone. Regarding precipitation, the rainy years of 1989 and 2019 stand out, as high pluviometric fragility zones occurred in ILs and PPAs. Despite static geo-environmental variables not favoring this, in 2019, deforestation points were observed within the boundaries of ILs, which could intensify the climatic impacts of AD^- through extreme rainfall. However, despite this study focusing on the annual scale of precipitation and emphasizing rainy and dry years, it is known that the region of GRW experiences a seasonal pattern marked by the rainy season in the first semester and the dry season in the second semester (Kubota et al., 2019). Under these conditions, a seasonal approach may show more pronouncedly the spatial difference in pluviometric fragility during the rainy season under the effects of LN and AD^-, and during the dry season influenced by EN and AD^+.

Rodrigues et al. (2020) analyzed an extreme rainfall event in 2018 in the municipality of Paragominas (eastern GRW), where there was high pluviometric intensity. Pedreira Júnior et al. (2020) described in their scientific paper that climatic phenomena such as LN events increase the frequency and intensity of storms in the Amazon region, implying greater erosive potential on the soil. This observation was also made by Costa and Blanco (2018) in their studies, where they found that LN and AD^- were related to higher erosion indices in the northern Amazon. Such information is crucial for confirming that these natural events are capable of enhancing HF increase in the Amazon. Thus, reports like these complement the analysis of this study, as the GRW region is marked by deforestation for agricultural purposes, making the soil more vulnerable to erosive processes, as the reduction in forest cover exposes the soil to the impacts of heavy rainfall (Li and Fang, 2016; Sarapatka and Bednar, 2022).

Furthermore, the deforestation zones detected in this study are alarming as they involve serious socio-environmental issues, such as encroachment on areas protected by laws. From a social perspective, it is evident the expansion of the agricultural frontier over the years analyzed, since 2012, towards the areas of ILs, where pastures were observed in all scenarios that have only increased over time. Bowman et al. (2021) also reported similar observations in their research, noting that the Amazon rainforest undergoes a slow process of environmental degradation in protected indigenous areas due to deforestation. These findings corroborate the results observed in GRW, where some points of medium HF were detected within ILs. It is worth noting that there are more points of medium HF observed in LN and AD^- years, indicating that despite deforestation contributing to the increase in HF, the high volume of precipitation in extreme years exacerbates this degradation.

From an environmental perspective, the accelerated deforestation observed every year, also considering within the boundaries of PPAs, CUs, and ILs, can lead to serious environmental problems. In this regard, unsustainable removal of vegetation has severe consequences, such as increased soil erosion (Teshome et al., 2022). The causes of this deforestation are related to the intensification of pasture activities and the expansion of soybean cultivation in the western part of GRW (Fuchs, 2020; Pinillos et al., 2021). This scenario contributes to significant environmental impacts, as the removal of natural vegetation reduces evapotranspiration and, consequently, rainfall recharge (Llopart et al., 2018; Leite-Filho et al., 2021). Another environmental harm due to uncontrolled soy-driven deforestation is the water deficit, as soy requires a large amount of water for its maintenance and production (Volken et al., 2022), which can affect the river system (Yasarer et al., 2020). Considering this information, the advance of soy and pasture near the source of the Gurupi River and throughout its surroundings is concerning, once it jeopardizes regional water availability and could even impact agriculture.

These findings are relevant given the expansion of reforestation during the analyzed period in GRW, which was concentrated in the GU. This sector of GRW potentially carries a higher risk due to the dominance of static geo-environmental variables that favor terrain instability. It is important to note that fluvial fragility is the only static geo-environmental variable (for calculation purposes) in the analysis that has a seasonal dynamic, as it depends directly on rainfall variability. In other words, during rainy periods, there is a tendency for larger areas of fluvial fragility, while during droughts, the values tend to decrease. Therefore, since its cartography is derived from the drainage network, there are no spatial data on rivers by year, so it is recommended to consider static fluvial fragility only in theoretical terms.

In light of these situations, the detection and analysis of HF in GRW serve as a basis for the formulation of environmental plans and policies, and is essential for better watershed management (Narendra et al., 2021). Pressure from agriculture has been identified in recent years in PPAs, CUs, and ILs in GRW. This issue can be addressed through sustainable alternatives such as a soy moratorium (Paim, 2021), agricultural zoning (Marin et al., 2022), and agroforestry and polyculture systems (Bowman et al., 2021). Bowman et al. (2021) also emphasized that the measures proposed in their research have additional advantages for environmental conservation, such as the restoration of degraded areas, prevention of deforestation of planted forests, increased biodiversity, and higher profitability in agroforestry cases. The discussed and detected reforestation is crucial in stabilizing these naturally unstable areas, which can be exacerbated in extreme years associated with deforestation.

Conclusions

Precipitation in GRW exhibits high spatiotemporal variability, particularly during extreme years, leading to the temporary

emergence (period of activity and impact of phenomena) of highly vulnerable areas due to prolonged and intense rainfall induced by AD^- and LN events. Conversely, stability in fragility occurs when climatic phenomena inhibit precipitation, such as in the case of AD^+ and EN events. There is an ongoing process of deforestation in GRW as agricultural frontiers encroach upon protected areas, which is a concerning sign, especially in the western sector where there is a greater concentration of soybean and pasture-related agriculture activities. This expansion of the agricultural frontier serves as a warning for the southern sector of GU. If deforestation continues at this pace, regional ecosystems will likely suffer even greater environmental impacts, including alterations in GRW hydrological patterns, particularly endangering the Gurupi River's source.

GRW is dominated by static geo-environmental variables that favor high terrain instability, rendering its natural state extremely fragile. This underscores the importance of forest control and conservation practices since soil erosion can negatively impact environmental and socioeconomic sectors due to soil loss and reduced quality for crop cultivation. Furthermore, this naturally unstable scenario can be exacerbated by accelerated deforestation in conjunction with extreme climatic events.

Differences in HF (fragility hazard assessment) were observed in certain areas of GRW. In extreme years characterized by precipitation surplus in a scenario of greater forest conservation, HF is more influenced by the effects of natural events and static geo-environmental variables. However, as agro-pastoral expansion intensifies, deforestation starts to have a greater impact on HF. A third, more critical scenario arises in extremely rainy years associated with extensive forest cover removal, resulting in high HF in GRW.

Given that extreme years are factors beyond human control, actions focused on sustainable conservation and preservation practices regarding LULC may be viable for mitigating the impacts of deforestation. Some of these actions may be within the scope of conservation policies. Property environmental records and soy moratoriums are means to curb uncontrolled deforestation and can provide regional natural resource managers with guidance for mitigating both climatic and anthropogenic pressures on GRW.

Acknowledgments

Fundação Amazônia de Amparo a Estudos e Pesquisas – FAPESPA (Amazon Foundation for Studies and Research Support). Research group of Núcleo de Pesquisa Aplicada ao Desenvolvimento Regional – NUPAD (Center for Applied Research to Regional Development).

Contribution of authors:

GOMES, D.J.C.: Conceptualization, Data curation, Formal Analysis, Funding, acquisition, Investigation, Methodology, Resources, Software, Supervision, Validation, Visualization, Writing – original draft, Writing – review & editing. BELTRÃO, N.E.S.: Data curation, Formal Analysis, Resources, Validation, Visualization, Writing – review & editing. LIMA, A.M.M: Data curation, Formal Analysis, Resources, Validation, Visualization, Writing – review & editing

References

Agência Nacional de Águas e Saneamento Básico (ANA), 2015. Conjuntura dos recursos hídricos no Brasil: regiões hidrográficas brasileiras – edição especial. Brasília: ANA (November 01, 2022) at:. https://www.snirh.gov.br/portal/centrais-de-conteudos/conjuntura-dos-recursos hidricos/regioeshidrograficas2014.pdf/view

Agência Nacional de Águas e Saneamento Básico (ANA), 2022. Sistema Nacional de Informações sobre Recursos Hídricos (Accessed November 04, 2022) at:. https://www.snirh.gov.br/hidroweb/serieshistoricas

Aguirre-Ayerbe, I.; Merino, M.; Aye, S.L.; Dissanayake, R.; Shadiya, F.; Lopez, C.M., 2020. An evaluation of availability and adequacy of multi-hazard early warning systems in Asian countries: A baseline study. International Journal of Disaster Risk Reduction, v. 49, 1-11. https://doi.org/10.1016/j.ijdrr.2020.101749

Bacani, V.M.; Sakamoto, A.Y.; Luchiari, A.; Quénol, H., 2015. Sensoriamento remoto e SIG aplicados à avaliação da fragilidade ambiental de bacia hidrográfica, Mercator, v. 14, (2), 119-135. https://doi.org/10.4215/RM2015.1402.0008

Bowman, K.W.; Dale, S.A.; Dhanani, S.; Nehru, J.; Rabishaw, B.T., 2021. Environmental degradation of indigenous protected areas of the Amazon as a slow onset event. Current Opinion in Environmental Sustainability, v. 50, 260-271. https://doi.org/10.1016/j.cosust.2021.04.012

Climate Hazards Group InfraRed Precipitation with Stations (CHIRPS), 2022. Rainfall estimates from gauge and satallite observation. Climate Hazards Center, UC Santa Bárbara (Accessed October 09, 2022) at:. https://data.chc.ucsb.edu/products/CHIRPS-2.0/

Companhia de Pesquisa de Recursos Minerais (CPRM), 2022. Serviço Geológico Brasileiro. Dados, Informações e Produtos (Accessed October 12, 2022) at:.https://geosgb.cprm.gov.br/geosgb/downloads.html

Córdova, M.; Célleri, R.; Delden, A., 2022. Dynamics of precipitation anomalies in Tropical South America. Atmosphere, v. 13, (6), 1-13. https://doi.org/10.3390/atmos13060972

Costa, C.A.A.; Blanco, C.J.C., 2018. Influência da variabilidade climática sobre a erosividade em Belém (PA). Revista Brasileira de Meteorologia, v. 33, (3), 509-520. https://doi.org/10.1590/0102-7786333010

Dias, F.G.; Lima, A.M.M., 2020. Zoneamento hidroambiental da bacia hidrográfica do rio Acará, Amazônia Oriental. Caderno de Geografia, v. 30, (61), 431-450. https://doi.org/10.5752/P.2318-2962.2020v30n61p450

Empresa Brasileira de Pesquisas Agropecuárias (EMBRAPA), 2022. Sistema Brasileiro de Classificação de Solos (SiBCS) (Accessed October 11, 2022) at:. http://geoinfo.cnps.embrapa.br/layers/?limit=100&offset=0

Faisal, B.M.R.; Hayakawa, Y.S., 2022. Geomorphological processes and their connectivity in hillslope, fluvial, and coastal areas in Bangladesh: A

review. Progress in Earth and Planetary Science, v. 9, (41), 1-22. https://doi.org/10.1186/s40645-022-00500-8

França, L.C.J.; Lopes, L.F.; Morais, M.S.; Lisboa, G.S.; Rocha, S.J.S.S.; Morais Junior, V.T.M.; Santana, R.C.; Mucida, D.P., 2022. Environmental Fragility Zoning using GIS and AHP modeling: perspectives for the conservation of natural ecosystems in Brazil. Conservation, v. 2, (2), 349-366. https://doi.org/10.3390/conservation2020024

Fuchs, V.B., 2020. Chinese-drive frontier expansion in the Amazon: four axes of pressure caused by the growing demand for soy trade. Revista Ciências Sociais, v. 20, (1), 16-31. https://doi.org/10.15448/1984-7289.2020.1.34656

Funk, C.; Peterson, P.; Landsfeld, M.; Pedreros, D.; Verdin, J.; Shukla, S.; Husak, G.; Rowland, J.; Harrison, L.; Hoell, A.; Michaelsen, J., 2015. The climate hazards infrared precipitation with stations – a new environmental record for monitoring extremes. Scientific data, v. 2, (150066), 1-21. https://doi.org/10.1038/sdata.2015.66

Gomes, D.J.C.; Nascimento, M.M.M.; Pereira, F.M.; Dias, G.F.M.; Meireles, R.R.; Souza, L.G.N.; Picanço, A.R.S.; Ribeiro, H.M.C., 2022. Flow variability in the Araguaia river hydrographic basin influenced by precipitation in extreme years and deforestation. Brazilian Journal of Environmental Sciences (RBCIAMB), v. 57, (3), 451-466. https://doi.org/10.5327/Z2176-94781358

Huguenin, L.; Meirelles, R.M.S., 2022. Do período colonial à COP26: breve resgate histórico sobre as mudanças climáticas relacionadas ao uso da terra no Brasil. Revista Brasileira de Educação Ambiental, v. 17, (5), 132-149. https://doi.org/10.34024/revbea.2022.v15.13930

Instituto Brasileiro de Geografia Física (IBGE), 2022. Geociências – Informações Ambientais (Accessed October 10, 2022) at:. https://www.ibge.gov.br/geociencias/informacoes-ambientais/geomorfologia.html

Instituto Nacional de Meteorologia (INMET), 2022. Normais Climatológicas (Accessed August 19, 2022) at:. https://clima.inmet.gov.br/NormaisClimatologicas/1961-1990/precipitacao_acumulada_mensal_anual.

Instituto Nacional de Pesquisas Espaciais (INPE), 2022 (Accessed August 10, 2022) at:. http://www.webmapit.com.br/inpe/topodata/

Jahfer, S.; Vinayachandran, P.N.; Nanjundiah, R.S., 2017. Long-term impacto of Amazon River runoff on northern hemispheric climate. Scientific Reports, v. 7, (10989), 1-9. https://doi.org/10.1038/s41598-017-10750-y

Jorge, R.L.O.; Lucena, D.B., 2018. Eventos extremos anuais de precipitação em Mauriti- CE. Ciência & Natura, v. 40, (65), 1-10. https://doi.org/10.5902/2179460X34045

Kelman, I., 2019. Pacific island regional preparedness for El Niño. Environmental, Development and Sustainability, v. 21, 405-428. https://doi.org/10.1007/s10668-017-0045-3

Kubota, N.A.; Prata, T.C.; Lima, I.F.; Lima, A.M.M., 2019. Hidrogeomorfologia e susceptibilidade a erosão da bacia do rio Gurupi (PA-MA). Revista Geográfica Acadêmica, v. 13, (2), p. 67-89. ISSN 1678-7226

Leite-Filho, A.T.; Soares-Filho, B.S.; Davis, J.L.; Abrahão, G.M., 2021. Deforestation reduces rainfall and agricultural revenues in the Brazilian Amazon. Nature Communications, v. 12, (2591), 1-7. https://doi.org/10.1038/s41467-021-22840-7

Li, Z.; Fang, H., 2016. Impacts of climate change on water erosion: a review. Earth-Science Reviews, v. 163, 94-117. https://doi.org/10.1016/j.earscirev.2016.10.004

Lira, K.C.S.; Francisco, H.R.; Feiden, A., 2022. Classification of environmental fragility in watershed using Fuzzy logic and AHP method. Sociedade & Natureza, v. 34, 1-17. https://doi.org/10.14393/SN-v34-2022-62872

Llopart, M.; Reboita, M.S.; Coppola, E.; Giorgi, F.; Rocha, R.P.; Souza, D.O., 2018. Land use change over the Amazon forest and its impact on the local climate. Water, v. 10, (2), 1-12. https://doi.org/10.3390/w10020149

Marengo, J.A.; Jimenez, J.C.; Espinoza, J.; Cunha, A.P.; Aragão, L.E.O., 2022. Increased climate pressure on the agriculture frontier in the Eastern Amazonia-Cerrado transition zone. Scientific Reports, v. 12, (457), 1-10. https://doi.org/10.1038/s41598-021-04241-4

Marin, F.R.; Zanon, A.J.; Monzon, J.P.; Andrade, J.F.; Silva, E.H.F.M.; Richter, G.L.; Antolin, L.A.S.; Ribeiro, B.S.M.R.; Ribas, G.G.; Battisti, R.; Heinemann, A.B.; Grassini, P., 2022. Protecting the Amazon forest and reducing global warming via agricultural intensification. Nature Sustainability, v. 5, 1018-1026. https://doi.org/10.1038/s41893-022-00968-8

Musso, A.; Tikhomirov, D.; Plotze, M.L.; Greinwald, K.; Hartmann, A.; Geitner, C.; Maier, F.; Petibon, F.; Egli, M., 2022. Soil formation and mass redistribution during the Holocene using meteoric ^{10}Be, soil chemistry and mineralogy, Geosciences v. 12, (2), 1-42. https://doi.org/10.3390/geosciences12020099

Narendra, B.H.; Siregar, C.A.; Dharmawan, W.S.; Sukmana, A.; Pratiwi; Pramono, I.B.; Basuki, T.M.; Nugroho, H.Y.S.H.; Supangat, A.B.; Purwanto; Setiawan, O.; Nandini, R.; Ulya, N.A.; Arifanti, V. B.; Yuwati, T.W., 2021. A review on sustainability of watershed management in Indonesia. Sustainability, v. 13, (19), 1-29. https://doi.org/10.3390/su131911125

Nóbrega, R.S.; Santiago, G.A.C.F.; Soares, D.B., 2016. Tendências do controle climático oceânico sob a variabilidade temporal da precipitação no Nordeste do Brasil. Revista Brasileira de Climatologia, v. 18, 276-292. https://doi.org/10.5380/abclima.v18i0.43657

Paca, V.H.M.; Espinoza-Dávalos, G.E.; Moreira, D.M.; Comair, G., 2020. Variability of trends in precipitation across the Amazon River basin determined from the CHIRPS precipitation product and from station records. Water, v. 12, (5), 1-22. https://doi.org/10.3390/w12051244

Paim, M., 2021 Zero deforestation in the Amazon: the soy moratorium and global forest governance. Review of European, Comparative & International Environmental Law, v. 30, (2), 220-232. https://doi.org/10.1111/reel.12408

Pedreira JÚnior, A.L.; Querino, C.A.S.; Biudes, M.S.; Machado, N.G.; Santos, L.O.F.; Ivo, I.O., 2020. Influence of El Niño and La Niña phenomena on seasonality of the relative Frequency of rainfall in southern Amazonas mesoregion. Revista Brasileira de Recursos Hídricos, v. 25, (24), 1-8. https://doi.org/10.1590/2318-0331.252020190152

Pezzi, L.P.; Souza, R.B.; Quadro, M.F.L., 2016. Uma revisão dos processos de interação oceano-atmosfera em região de intenso gradiente termal do oceano Atlântico Sul baseada em dados observacionais. Revista Brasileira de Meteorologia, v. 31, (4), 428-453. https://doi.org/10.1590/0102-778631231420150032

Pinillos, D.; Poccard-Chapuis, R.; Bianchi, F.J.J.A.; Corbeels, M.; Timler, C.J.; Tittonell, P.; Ballester, M.V.R.; Schulte, R.P., 2021. Landholderss' perceptions on legal reserves and agricultural intensification: diversity and implications for forest conservation in the Eastern Brasilian Amazon. Forest Policy and Economics, v. 129, 1-14. https://doi.org/10.1016/j.forpol.2021.102504

Projeto MapBiomas, 2022. 2022 – Coleção 7 da série anual de mapas de cobertura e uso do solo do Brasil (Accessed October 08, 2022) at:. https://mapbiomas.org/

Rodrigues, R.S.S.; Silva, M.N.A.; Ferreira Filho, D.F.; Bezerra, P.E.S.; Figueiredo, N.M., 2020. Análise dos efeitos de um evento extremo de chuva sobre o escoamento superficial em uma pequena bacia hidrográfica rural amazônica. Revista Brasileira de Climatologia, v. 26, 368-392. https://doi.org/10.5380/abclima.v26i0.65246

Ross, J.L.S., 1994. Análise empírica da fragilidade dos ambientes naturais e antropizados. Revista do Departamento de Geografia, v. 8, 3-74. https://doi.org/10.7154/RDG.1994.0008.0006

Saaty, T.L., 1980. The analytic Hierarchy Process. McGraw-Hill, New York. Scientific Research an Academic Publisher (Accessed December 02, 2022) at:. https://www.scirp.org/(S(lz5mqp453edsnp55rrgjct55))/reference/ReferencesPapers.aspx?ReferenceID=1943982

Sarapatka, B.; Bednar, M., 2022. Rainfall erosivity impacts on sustainable management of agricultural land in changing climate conditions. Land, 11, (4), 1-11. https://doi.org/10.3390/land11040467.

Silva, L.F.; Battazza, A.; Souza, N.F.; Fagundes, N.; Souza, D.; Rocha, N.S., 2022. Impactos das ações antrópicas aos biomas do Brasil: artigo de revisão. Meio Ambiente (Brasil), v. 4, (1), 21-44. ISSN: 2675-3065

Silva, T.C.M.; Vieira, I.C.G.; Thalês, M.C., 2021. Spatial-temporal evolution of landscape degradation on the Guamá river basin, Brazil. Brazilian Journal of Environmental Sciences (RBCIAMB), v. 56, (3), 480-490. https://doi.org/10.5327/Z21769478942

Sinshaw, B G.; Belete, A.M.; Tefera, A.K.; Dessie, A.B.; Bizuneh, B.B.; Alem, H.T.; Atanaw, S.B.; Eshete, D.G.; Wubetu, T.G.; Atinkut, H.B.; Moges, M.A., 2021. Prioritization of potential soil erosion susceptibility region using fuzzy logic and analytical hierarchy process, Upper Blue Nile basin, Ethiopia. Water-Energy Nexus, v. 4, 10-24. https://doi.org/10.1016/j.wen.2021.01.001

Siqueira, R.G.; Lima, V.C.; Souza, J.J.L.L. 2017. Análise quantitativa da variabilidade espacial da densidade de drenagem com o estimador de densidade de Kernel em ambiente SIG. Anais do XVIII Simpósio Brasi\leiro de Sensoriamento Remoto, 28-31 de Maio de 2017, INPE, Santos-SP (Accessed November 11, 2022) at:. https://proceedings.science/sbsr/papers/analise-quantitativa-da-variabilidade-espacial-da-densidade-de-drenagem-com-o-estimador-de-densidade-de-kernel-em-ambien?lang=pt-br

Teshome, D.S.; Moisa, M.B.; Gemeda, D.O.; You, S., 2022. Effect of land use-land cover change on soil erosion and sediment yield in Muger sub-basin, Upper Blue Nile basin, Ethiopia. Land, v. 11, (12), 1-20. https://doi.org/10.3390/land11122173

Towner, J.; Cloke, H.L.; Lavado, W.; Santini, W.; Bazo, J.; Perez, E.C.; Stephens, E.M., 2020. Attribution of Amazon floods to modes of climate variability: a review. Meteorological Applications, v. 27, (5), 1-36. https://doi.org/10.1002/met.1949

Tricart, J., 1977. Ecodynamics (Accessed December 01, 2022) at:. http://biblioteca.ibge.gov.br/visualizacao/monografias/GEBIS-RJ/ecodinamica.pdf

Volken, N.J.; Minoti, R.T.; Alves, C.M.A.; Vergara, F.E., 2022. Analyzing the impact of agricultural water-demand management on water availability in the Urubu river basin – Tocantins, Brazil. Ambiente & Água – An Interdisciplinary Journal of Applied Science, v. 17, (4), 1-23. https://doi.org/10.4136/ambi-agua.2847

Yasarer, L.M.W.; Taylor, J.M.; Rigby, J.R.; Locke, M.A., 2020. Trends in land use, irrigation, and streamflow alteration in the Mississippi river alluvial plain. Frontiers in Environmental Science, v. 8, (66), 1-13. https://doi.org/10.3389/fenvs.2020.00066